We are IntechOpen, the world's leading publisher of Open Access books
Built by scientists, for scientists

4,800
Open access books available

122,000
International authors and editors

135M
Downloads

Our authors are among the

154
Countries delivered to

TOP 1%
most cited scientists

12.2%
Contributors from top 500 universities

CLARIVATE ANALYTICS
BOOK CITATION INDEX
INDEXED

WEB OF SCIENCE™

Selection of our books indexed in the Book Citation Index in Web of Science™ Core Collection (BKCI)

Interested in publishing with us?
Contact book.department@intechopen.com

Numbers displayed above are based on latest data collected.
For more information visit www.intechopen.com

Chapter 5

Decomposition Mechanisms of BODIPY Dyes

Yuriy S. Marfin, Sergey D. Usoltsev and
Evgeniy V. Rumyantsev

Additional information is available at the end of the chapter

http://dx.doi.org/10.5772/intechopen.80498

Abstract

The stability of metal complexes in both thermodynamic and kinetic aspects always was a matter of interest in the field of coordination chemistry. Practical implementation of a fluorophores in a field of molecular biology also is essentially constrained by their solvolytic and protolytic stability. The aforementioned emphasizes interest in a search for factors of quantitative stability-based discrimination on a row of BODIPY derivatives. This chapter shows that thermodynamic stability of a dipyrrinates varies to a large extent from a mostly undestructable solvolytically BODIPYs to a very volatile in the same aspect rare-earth element complexes.

Keywords: BODIPY, decomposition mechanisms, stability, acidic conditions, kinetic data, dissociation

1. Introduction

The stability of metal complexes in both thermodynamic and kinetic aspects always was a matter of interest in the field of coordination chemistry. Whereas the thermodynamical approach to investigation of coordination compound stability was well established back before the first half of the twentieth century [1, 2], there were very few, if any, attempts to systematize patterns of formation and destruction of complexes in a kinetical aspect.

A monograph published in 2007 [3] highlights the factors affecting kinetics of dissociation and mechanisms of this process for a vast range of coordination compounds. Both well-known 'Verner' complexes and the most contemporary porphyrinato and phthalocyaninato complexes are discussed therein. Remarkable contribution made to the topic by the authors was systematization of the factors, influencing both kinetic and thermodynamic stability of the

IntechOpen

© 2019 The Author(s). Licensee IntechOpen. This chapter is distributed under the terms of the Creative Commons Attribution License (http://creativecommons.org/licenses/by/3.0), which permits unrestricted use, distribution, and reproduction in any medium, provided the original work is properly cited. CC BY

complex compounds. Due to the universal nature of the proposed models, they could be easily adapted to describe dissociation processes taking place for other complexes. High impact of both external (selected solvent and reagent) and internal (molecular structure) parameters on the dissociation process, showed in the monograph, emphasizes importance of the study for pure and applied chemistry of the dipyrrins.

The process of optimisation of physicochemical properties of the compounds essentially implies a search for the compromise between the photophysical efficiency and stability. The latter, in turn, includes resilience to solvolytic, protolytic and solvoprotolytic dissociation and photochemical, thermooxidative and some other destruction routes [4, 5]. Our research shows that thermodynamic stability of a dipyrrinate varies to a large extent from a mostly undestructable solvolytically BODIPYs to a very volatile in the same aspect rare-earth element complexes. Work of our colleagues from Tomsk [6–8] shows that immobilization of a BODIPY in a sol–gel silicon oxide involves specific interactions of a chromophore with a silanol moiety of a matrix. This drastically influences fluorescence quantum yield of the chromophore, decreasing it up to a factor of 100 and causing significant changes in the shape of both fluorescence and absorbance spectrum. Interestingly, a similar behaviour is observed for BODIPY upon interaction with protic solvents and Arrhenius acids. The common thing in both situations is that sol–gel technology involves usage of aggressive medium on the early stages of either acid-catalysed process or a base-catalysed one [9]. Research [10] shows decrease of pH to affect BODIPY photophysical parameters in an irreversible manner. Namely, HCl addition in ethanol causes BODIPY destruction via $[BF_2]^+$ elimination, leading to a protonated form of dipyrromethene. Further development of a practically important process of a composite material elaboration obviously requires a careful study of stability of a fluorophore in an acid and basic media. Practical implementation of a fluorophore in a field of molecular biology also is essentially constrained by their solvolytic and protolytic stability. The aforementioned emphasizes interest in a search for factors of quantitative stability-based discrimination in a row of BODIPY derivatives.

Our collaboration with the Institute of Solution Chemistry of the Russian Academy of Sciences pushed the limits in the field thanks to the huge amount of data and experience in the studies of such processes for porphyrins and phthalocyanines. Until the current review on dipyrrinate stability, our colleagues from ISC RAS have published [11, 12] kinetics of $Cu(II)$, $Ni(II)$, $Co(II)$ and $Hg(II)$ dissociation processes in a benzene solution of acetic acid. Surprisingly, $Hg(II)$ complexes do undergo dissociation even in acid-free benzene and chloroform solutions. Such a process involves formation of $Hg \cdot Solv$ adducts alongside with protonated dipyrromethene via the stage of a π-complex formation:

$$[Hg(dpm)_2 + C_6H_6 \leftrightarrow \left[Hg(dpm)_2\right] \cdot C_6H_6 \leftrightarrow [C_6H_6 \cdots Hg \cdots dpm]^+ dpm^- \rightarrow [C_6H_5 - Hg - dpm]$$
$$[C_6H_5 - Hg - dpm] + C_6H_6 \rightarrow [C_6H_5 - Hg - C_6H_5] + Hdpm \tag{1}$$

Analysis of dissociation kinetics of other stated dipyrrinates in acetic acid benzene solutions yields a row of descending stability to protolytic dissociation:

$$\left[Cu(dpm)_2\right] > \left[Co(dpm)_2\right] \approx \left[Zn(dpm)_2\right] \gg \left[Hg(dpm)_2\right] \gg \left[Ni(dpm)_2\right] \quad (2)$$

Whereas this row coincides roughly with a respective row for thermodynamic stability, it has absolutely nothing to do with the corresponding dependencies for complexes of a structurally flexible chelate and amines like ethylenediamine. Stability of the $Ni(II)$ complex for porphyrins and phthalocyanines also occupies different positions in a corresponding row. Moreover, somehow, comparable destruction rate in such a condition is only observed for yet the most labile macrocyclic complex [13] being samarium(II) octaphenyltetraazaporphyrinate—$[(Acac)SmOPTAP]$. This $[(Acac)SmOPTAP]$ in benzene with 0.2 M $AcOH$ (303.15 K) has a $k_{obs} = 1.6 \cdot 10^{-4} s^{-1}$. $\left[Co(dpm)_2\right]$ and $\left[Zn(dpm)_2\right]$ in a similar condition (benzene, 0.33 M $AcOH$, 303.15 K) exhibit k_{obs} below $1.1 \cdot 10^{-4} s^{-1}$.

To summarize, available data demonstrates lack of macrocyclic effect in dipyrrinates to negatively impact complexes stability. Influence of this structural disadvantage is exemplified for the $Ni(II)$ complexes as stated above. At the same time, spatial rigidity as compared to diammines and similar chelates implies their distinct behaviour granting special interest in the field.

2. Protolytic dissociation of alkylated Zn (II) dipyrrinates

Here we review research on kinetics of $Zn(II)$ dipyrrinate $\left[Zn(dpm)_2\right]$ protolytic dissociation [14]. The structures discussed are presented below:

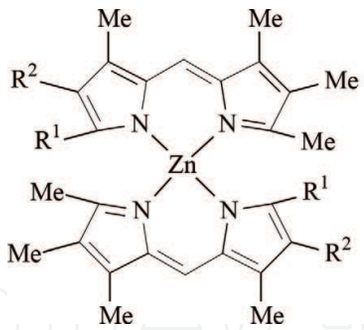

$$[Zn(dpm^1)_2]: R^1 = H, R^2 = Me$$
$$[Zn(dpm^2)_2]: R^1 = Me, R^2 = H$$
$$[Zn(dpm^3)_2]: R^1 = Me, R^2 = Et$$

$Zn(II)$ dipyrromethene complexes were shown to be quite perspective among other d-metal complexes, because due to fully occupied d-electron shell, no ligand fluorescence quenching occurs. It was found earlier [15] that $\left[Zn(dpm)_2\right]$ complexes are exposed to protolytic dissociation in C_6H_6–CH_3COOH solutions, so such a mixture was also used to study protolytic dissociation in this case.

Electronic absorption and fluorescence spectroscopy was used for examination of dissociation kinetics at 298, 308, 318 and 328 K temperature points. Observed rate constant (k_{obs}), activation energy (E_a) and entropy ($\Delta S^{\neq}$) were calculated as follows:

$$k_{obs} = \frac{1}{\tau} \cdot ln\left(\frac{A_0 - A_\infty}{A_\tau - A_\infty}\right) \quad (3)$$

where A_0, A_∞ and A_τ are absorbance in the first, intermediate and the last point, respectively.

$$E_a = 19.1 \cdot \frac{T_1 T_2}{T_2 - T_1} \cdot lg \frac{k^{T_2}}{k^{T_1}}, \qquad \Delta S^{\neq} = 19.1 \cdot lgk^T + E_a/T - 19.1 \cdot lgT - 205 \tag{4}$$

Electronic absorption spectra of the compounds exhibit bright characteristic absorption band at 500 nm corresponding to $S_0 \rightarrow S_1$ electronic transition and charge-transfer band at ~370 nm. Fluorescent bands are single-peak mirror images of the main absorption band.

It was shown, that addition of acetic acid in benzene provokes decrease of the long-wavelength absorption maximum (λ_{abs} = 497–506 nm) with a simultaneous increase pro rata in the 485–488 nm peak, corresponding to the protonated ligand form (H_2dpm^+). On the other side, a decrease in the main fluorescence band of the compound was not accompanied by any other changes which was in the good agreement with the fact that protonated dipyrromethene is not fluorescent (**Figure 1**).

It is reasonable to state, therefore, that $\left[Zn(dpm)_2\right]$ protolytic dissociation yields protonated ligand form—H_2dpm^+.

Even the smallest acid amounts provoked immediate $\left[Zn\left(dpm^1\right)_2\right]$ dissociation all the way to the equilibrium state. Data obtained from the experiments allowed us to measure protolytic dissociation equilibrium constant corresponding to the following scheme:

$$\left[Zn\left(dpm^1\right)_2\right] + 4HAcO = Zn(AcO)_2 + 2\left[H_2\left(dpm^1\right)^+ \cdots AcO^-\right] \tag{5}$$

Measured to be $5 \cdot 10^{-6} l^2/mol^2$, this constant is in the good agreement with existing data on thermodynamic stability of a similar complex [16].

Linearization of kinetic data for the $\left[Zn\left(dpm^3\right)_2\right]$ in the semi-logarithmic scale indicates first-order reaction relative to complex concentration (**Figure 2**). Dependence of the observable rate constant from the HAcO concentration could be written as

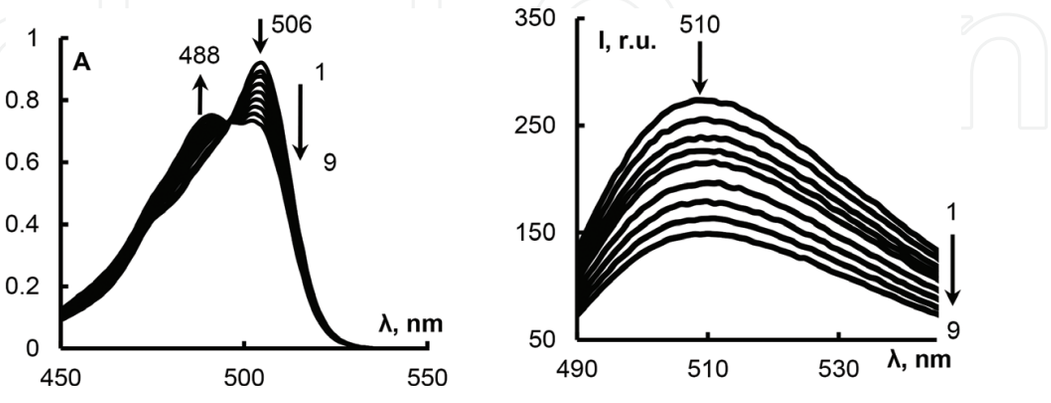

Figure 1. Left: changes in EAS of benzene [$Zn(dpm^3)_2$] solution upon *AcOH* addition (C = 0.78 *M*) (1—0 *min*; 9—30 *min*); and right: changes in [$Zn(dpm^2)_2$] benzene solution fluorescence upon *AcOH* addition (C = 0.7 *M*) (1—0 *min*; 9—30 *min*).

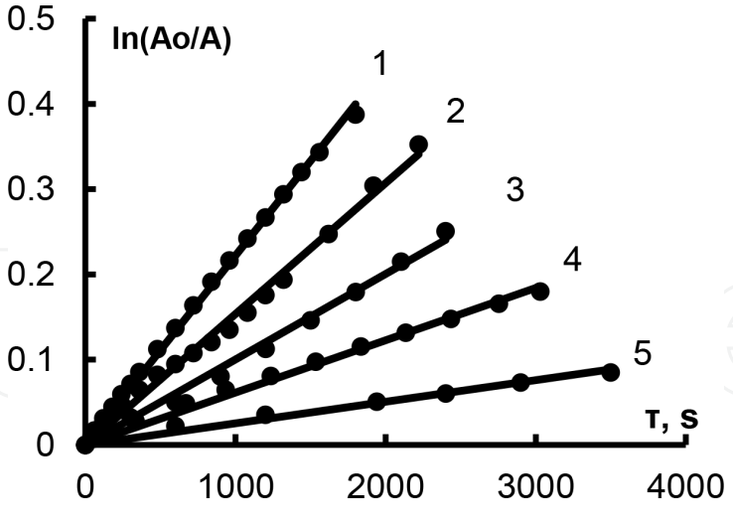

Figure 2. Kinetics of the $[Zn(dpm^3)_2]$ dissociation upon different *AcOH* concentrations (1—0.78 *M*; 2—0.67 *M*; 3—0.54 *M*; 4—0.39 *M*; and 5—0.21 *M*).

$$k_{obs} = kC_{HAcO}^2 \tag{6}$$

According to the literature data [17–19], Gammet's acidity function is in direct ratio with acid concentration in the range used (0.21–0.78 M); thus activity could be safely substituted with the concentration.

Protolytic dissociation, therefore, proceeds the same way as protonated ligand formation and could be described by the third-order kinetic equation:

$$-\frac{dC_{[Zn(dpm)_2]}}{d\tau} = k_{obs}C_{[Zn(dpm)_2]}C_{AcOH}^2 \tag{7}$$

Data obtained is in good agreement with the literature and justifies participation of two acid molecules in the limiting stage of the reaction. Analogous mechanism takes place in the protolytic dissociation of metalloporphyrins [20, 21], possessing similar structure of the coordination centre. Kinetic constant values k^T at different temperatures and corresponding activation parameters are presented below:

T, K	*k*, l²/(mol²·s)	E_a, kJ/mol	$\Delta S^{\neq}$, J/(mol·K)	$\Delta H^{\neq}$, kJ/mol
$[Zn(dpm^2)_2]$				
298	0.0001	61.2 ± 2.3	−119.6 ± 10.3	58.7 ± 2.2
308	0.0002			
318	0.0005			
$[Zn(dpm^3)_2]$				
298	0.0003	52.3 ± 3.2	−141.1 ± 12.4	49.8 ± 3.2
308	0.0005			
318	0.0007			

T, K	k, l²/(mol²·s)	E_a, kJ/mol	$\Delta S^{\neq}$, J/(mol·K)	$\Delta H^{\neq}$, kJ/mol
Zn(II) bis(4,4′-dibutyl-3,3′,5,5′-tetramethyl-2,2′-dipyrrinate)				
298	0.0006	51.4	−142.3	48.9
303	0.00099			
313	0.00171			
318	0.00232			

Formation of a protonated ligand form H_2L^+ and derived above third-order kinetic equations allows us to represent protolytic dissociation as the three-stage process of a consequent pyrrolic nitrogen protonation:

$$\begin{gathered}\left[Zn(dpm)_2\right] + 2HAcO \leftrightarrow \left\{\left[Zn(dpm)_2 \cdot 2H\right]^{2+} \cdots 2AcO^-\right\} \quad k_1, slow \\ \left\{\left[Zn(dpm)_2 \cdot 2H\right]^{2+} \cdots 2AcO^-\right\} \rightarrow 2Hdpm + Zn(AcO)_2 \quad k_2, fast \\ Hdpm + HAcO \rightarrow [H_2dpm^+ \cdots AcO^-] \quad k_3, fast\end{gathered} \tag{8}$$

With the quasi-steady-state assumption, the equation for $\left[Zn(dpm)_2\right]$ could be rewritten as:

$$-\frac{dC_{\left[Zn(dpm)_2\right]}}{d\tau} = \left(\frac{k_1 k_2}{k_{-1} + k_2}\right) C_{\left[Zn(dpm)_2\right]} C_{HAcO}^2 \tag{9}$$

which coincides with the experimentally derived equation. Further simplification is possible with the assumption of kinetic insignificance of k_{-1} due to low inverse reaction rate:

$$-\frac{dC_{\left[Zn(dpm)_2\right]}}{d\tau} = k_1 C_{\left[Zn(dpm)_2\right]} C_{HAcO}^2 \tag{10}$$

The rate-determining step is, therefore, the first stage. Activation parameters obtained serve as the further approval for the conclusions stated above. Namely, increase in ordering due to formation of $\left\{\left[Zn(dpm)_2 \cdot 2H\right]^{2+} \cdots 2AcO^-\right\}$ intermediate is described by the negative values of activation entropy.

Data presented allows us to identify the effects of dipyrrolic ligand alkyl substitution to the kinetic stability of the corresponding complexes for the first time. Whereas the α-free complex was shown to be of the highest lability, it is obvious to assume the high impact of +I effect existing therein to be the most important stabilizing factor. This assumption is supported by the proposed mechanism: $\left\{\left[Zn(dpm)_2 \cdot 2H\right]^{2+} \cdots 2AcO^-\right\}$ stability is determined solely by the strength of N-H hydrogen bonds. Decrease in +I effect impact along with fast emergence of steric difficulties leads to severe weakening of those bonds upon alkyl chain elongation (literature data for dibutyl-substituted dipyrromethene [15] was also used for comparison). Methyl group, in turn, provides the highest inductive impact as compared to related sterical

http://dx.doi.org/10.5772/intechopen.80498

difficulties—such a combination granting the lowest activation energy qualitatively represented by instant hydrolysis.

In our other paper [14], the search for analogies in photochemical and protolytic stability was performed.

Photochemical destruction processes of $\left[Zn\left(dpm^1\right)_2\right]$, $\left[Zn\left(dpm^2\right)_2\right]$ and $\left[Zn\left(dpm^3\right)_2\right]$ along with free dipyrromethene ligand and dipyrromethene hydrofluoride in ethanol were studied. OUFB-04 (180–275 nm, 11.4 W/m^2) was used, and observable destruction constants were evaluated from spectral changes at different time points (**Figure 3**). ^{1}H NMR spectra of the compounds were acquired using Bruker AVANCE-500 (Germany) spectrometer.

From the data obtained, we state the main role of oxidative hydroxylation of alkyl moieties and μ-carbon in the destruction process, yielding monopyrrolic products. Nuclear magnetic resonance spectroscopy data after irradiation indicates peaks, associated with $HO-CH_2-Pyr$ and alike moieties: ^{1}H NMR (500 MHz, $CDCl_3$) δ, ppm—1.25, 3.74, 7.39, 7.49 and 8.01.

Observable constants were measured to be $(8 \pm 3) \cdot 10^{-2}$, $(3.4 \pm 0.5) \cdot 10^{-2}$ and $(10 \pm 3) \cdot 10^{-2}$, respectively. Photolysis speed, therefore, grows in direct proportion with 'alkylation degree', and β-substituent affects this process much more intensively than the α one. Observable constants for free dipyrromethene and dipyrromethene hydrofluoride were measured to be $(16.7 \pm 0.9) \cdot 10^{-2}$ and $(8 \pm 2) \cdot 10^{-2}$, respectively. As it was expected, free of any acid–base and coordinational interactions, dipyrrin structure becomes way more labile to photodestruction due to high electron density allocated at the π-conjugated system.

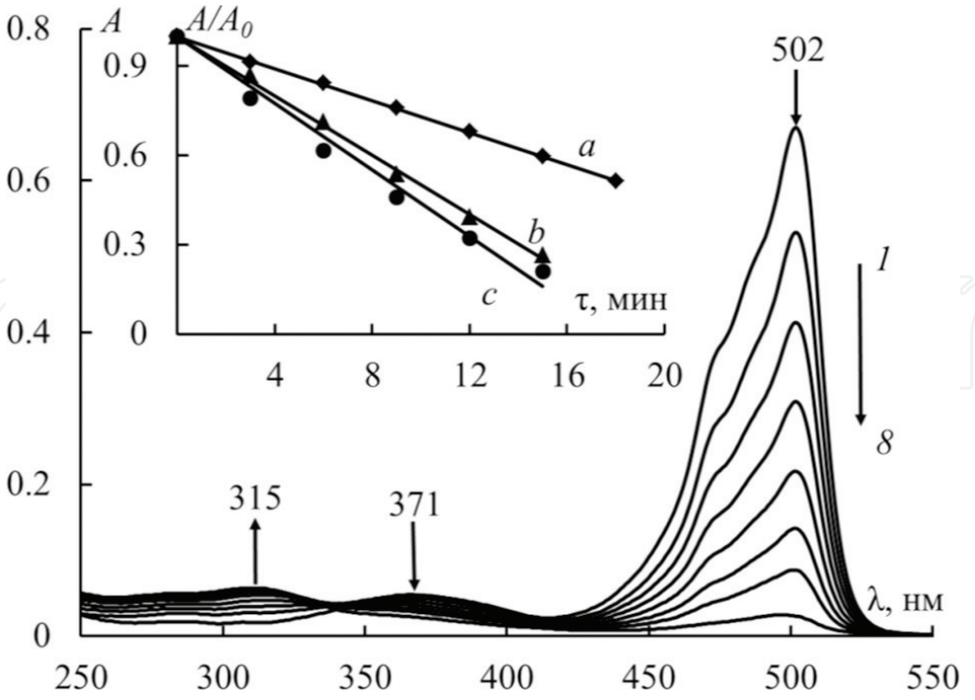

Figure 3. Changes in $[Zn(dpm^3)_2]$ ethanol solution EAS upon irradiation (1—0 *min*; 8—24 *min*); inset—relative optical density of the compounds upon irradiation (*a*—$[Zn(dpm^2)_2]$; b—$[Zn(dpm^1)_2]$; c—$[Zn(dpm^3)_2]$).

3. Protolytic dissociation of Pd(II) dipyrrinates and bis-dipyrrinates

Dipyrromethene ligands are known to possess flat molecular shape and mobile π-electron system. Such properties essentially suggest high interest in research concerning their DNA intercalating activity for anticancer purposes. The most promising complexes in this area are $Pt(II)$ and $Pd(II)$ organic coordination compounds, due to their flat square coordination polyhedra, perfect for fitting the molecule between nitrogenous bases. Unlike 3d-metal dipyrrinates, there are very few investigations carried out on their 4d analogues. There is also a high fundamental interest in comparative studies of the physicochemical properties for compounds with similar coordination environment but different ligand structures. Differences between dipyrrin and billadiene complexes are interesting object for the investigation; the latter possess additional chelating cycle, which provokes emergence of the differential polychelating effect [22].

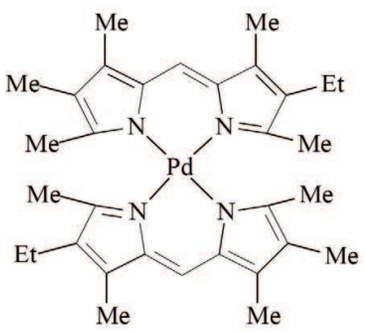

[Pd(dpm)$_2$]

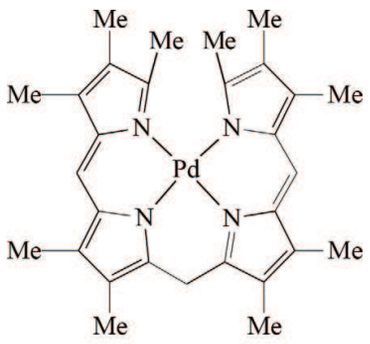

[Pd(bd)]

Here we review our research on $Pd(II)$ complexes with alkylated dipyrromethene ($Hdpm$) and billadiene-a,c (H_2bd).

Preliminary examination revealed absolute insusceptibility of the studied complexes to protolysis in C_6H_6–$AcOH$ solution. $Pd(II)$ complexes are, therefore, way more stable to protolytic dissociation than the 3d-metal dipyrrinates. Trichloroacetic acid benzene solution showed measurable reaction rate at 298 K and therefore was used for further kinetic investigations. Emergence and gradual growth of 485 nm peak in electronic absorption spectra indicated formation of protonated ligand form upon complex destruction (**Figure 4**).

Linear dependencies obtained for data plotted in semi-logarithmic coordinates indicate first-order reaction relative to complex concentration. Observable rate constants, at the same time, suggest second-order reaction relative to CCl_3COOH concentration:

$$k_{obs} = kC^2_{CCl_3COOH} \tag{11}$$

Protolytic dissociation therefore could be described by the third-order equation, in a similar way as the ligand protonation process:

$$-\frac{dC_{[Pd(dpm)_2]}}{d\tau} = kC_{[Pd(dpm)_2]}C^2_{CCl_3COOH} \tag{12}$$

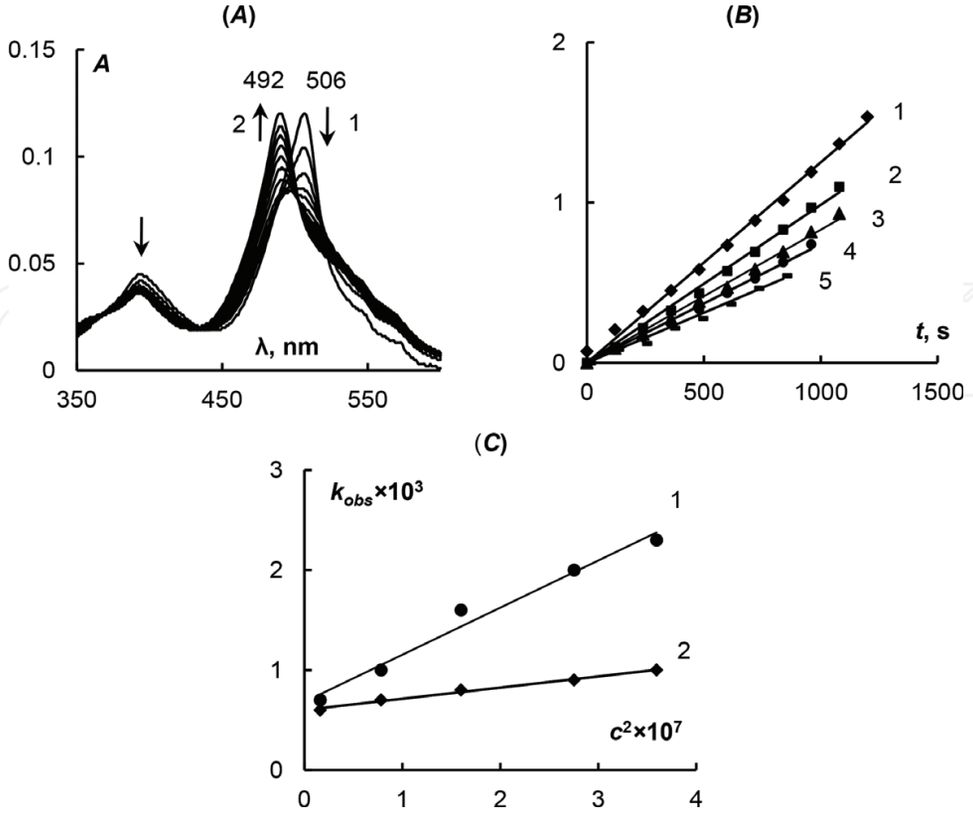

Figure 4. (A) Changes in [*Pd*(*bd*)] EAS upon protolytic dissociation 298.15 K; τ (s): 1—0 (s); 2—2820 (s); (B) kinetics of [*Pd*(*bd*)] dissociation at 298 K; $C^2_{CCl_3COOH} \cdot 10^4$; M: 6 (1), 5.3 (2), 4 (3), 2.8 (4), 1.3 (5); (C) dependence of k_{obs} from $C^2_{CCl_3COOH}$ (T = 298 K) for [*Pd*(*bd*)] (1) и [*Pd*(*dpm*)$_2$] (2).

$$-\frac{dC_{[Pd(bd)]}}{d\tau} = kC_{[Pd(bd)]}C^2_{CCl_3COOH} \tag{13}$$

Kinetical and activation parameters for the $Pd(II)$ complexes are listed below:

T, K	**k**	**E_a, kJ/mol**	**$\Delta S^{\neq}$, J/(mol·K)**	**$\Delta H^{\neq}$, kJ/mol**
[*Pd*(*dpm*)$_2$]				
298	4700 ± 200	52.4 ± 2.3	−6.0 ± 0.3	44.8 ± 2.2
308	7320 ± 360			
318	18,788 ± 393			
[*Pd*(*bd*)]				
298	1120 ± 50	65.8 ± 3.2	25.7 ± 0.5	65.3 ± 3.2
308	5210 ± 190			
318	5860 ± 280			

Formation of a protonated ligand form (H_2dpm^+ and H_4bd^{2+}) allows us to propose mechanism, analogical to the aforementioned bis-dipyrrinates dissociation scheme. Three-stage consequent nitrogen protonation reaction scheme is assumed:

$$\begin{gathered}\left[Pd(dpm)_2\right] + 2H^+\cdots A^- \leftrightarrow \left\{\left[Pd(dpm)_2 \cdot 2H\right]^{2+}\cdots 2A^-\right\}, \quad k_1, slow \\ \left\{\left[Pd(dpm)_2 \cdot 2H\right]^{2+}\cdots 2A^-\right\} \rightarrow 2Hdpm + PdA_2, \quad k_2, fast \\ Hdpm + H^+\cdots A^- \rightarrow [H_2dpm^+\cdots A^-], \quad k_3, fast\end{gathered} \tag{14}$$

Quasi-steady-state assumption for this process allows us to describe this process with the equation:

$$-\frac{dC_{\left[Pd(dpm)_2\right]}}{d\tau} = \left(\frac{k_1 k_2}{k_{-1} + k_2}\right) C_{\left[Pd(dpm)_2\right]} C^2_{H^+\cdots A^-}, \tag{15}$$

As it was done for $Zn(II)$ complexes before, simplification with the assumption of k_{-1} kinetical insignificance could be done to rewrite equation in a convenient form:

$$-\frac{dC_{\left[Pd(dpm)_2\right]}}{d\tau} = k_1 C_{\left[Pd(dpm)_2\right]} C^2_{H^+\cdots A^-} \tag{16}$$

Thus, the obtained activation parameters describe the transition state formation (rate-determining step). Here we also assume the possibility of interaction between the acid anion and Pd(II) atom.

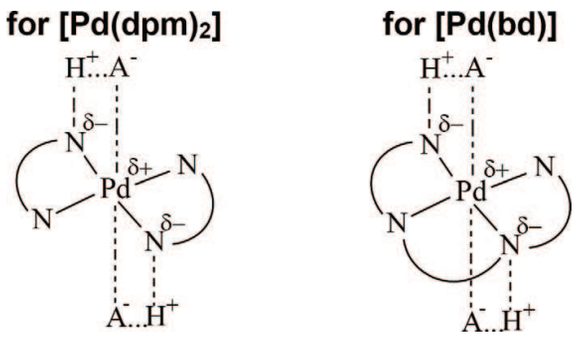

Comparison of the activation parameters for $\left[Pd(dpm)_2\right]$ and $[Pd(bd)]$ complexes suggests manifestation of differential polychelating effect, effectively screening coordination centre from external influence. Namely, observable dissociation rate constant is 4.2 times higher (T = 298 K) for bis-dipyrrinate than for billadiene complex, and activation energy of the limiting step is 1.3 times higher for the $[Pd(bd)]$.

It is worth mentioning here that in other researches, $Pt(III)$ billiverdine (natural billatriene) complex was found to be stable to protolysis in *DMSO-AcOH* solutions with up to 16.85 M acid concentration. At the same time, it dissociated instantly all the way to equilibrium state in $DMSO–H_2SO_4$ solutions. Data obtained for billiverdine and protoporphyrin IX complexes was used for evaluation of macrocyclic effect impact: kinetical stability increase measures 10^4 times for $Pt(III)$ protoporphyrinate. Macrocyclic effect was shown to significantly increase stability in the similar comparative study with the $Mn(III)$ complexes, where the stability increase was measured to be $1.73 \cdot 10^8$ times!

Both polychelating and macrocyclic effect should be therefore mentioned as the most important factors of coordination compound stabilization. The hallmark of these effects is a drastic decrease in dissociation rate constants upon switching from simply chelating ligands, to polychelating ones and, finally, to macrocyclic ligands.

4. Protolytic dissociation of Cu(II) and Ni(II) bis-dipyrrinates

Cu(*II*) and *Ni*(*II*) are known for their ability to form both biligand dipyrrinates $[M(dpm)_2]$ and a highly themodynamically stable heteroligand complexes $[Mdpm(X)]$. High stability of the latter (lg$K$ = 7–10) suggests formation of intermediate products with mixed coordination environment during protolytic dissociation process. This is indeed being the case for the *Cu*(*II*) complex with butyl-substituted dipyrromethene [23, 24].

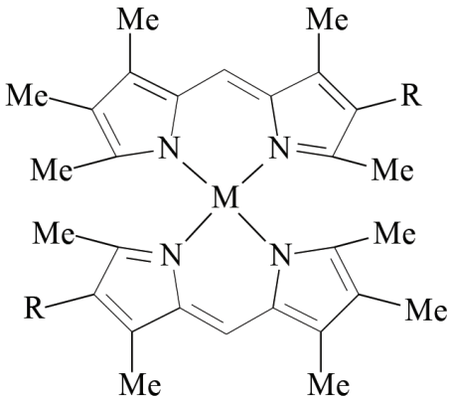

$$[Ni(dpm)_2]: M = Ni, R = Et$$
$$[Cu(dpm)_2]: M = Cu, R = Me$$

Investigation of *Cu*(*II*) and *Ni*(*II*) complexes protolytic dissociation was carried out to further understand influence of different factors on kinetic stability of dipyrrinates [15]. Benzolic $[Cu(dpm)_2]$ and $[Ni(dpm)_2]$ solutions possess three characteristic electronic absorption maxima: high-intensity one at 527–530 nm, second peak at 460–464 nm and the charge-transfer band in the near UV. The addition of a minimal AcOH amount was found to cause immediate intensity decrease for the main electronic absorption peak, accompanied by 488 nm peak emergence (**Figure 5**). Retaining of the spectral shape upon triethylamine addition approved this process to be reversible equilibrium. The thermodynamic equilibrium constant was obtained from the spectrophotometric titration data, assuming the process to be described with the equation below:

$$[Cu(dpm)_2] + 4AcOH = 2[H_2dpm](AcO) + Cu(AcO)_2 \quad (17)$$

Obtained thermodynamic constant value of $(7.55 \pm 0.4) \cdot 10^{-7} l^2/mol^2$ is in good agreement with the literature data on the *Cu*(*II*) dipyrrinate stability. Unlike the butyl-dipyrromethene complexes [15], our objects were found to exhibit not the formation of heteroligand compounds even when the smallest acid amounts were used.

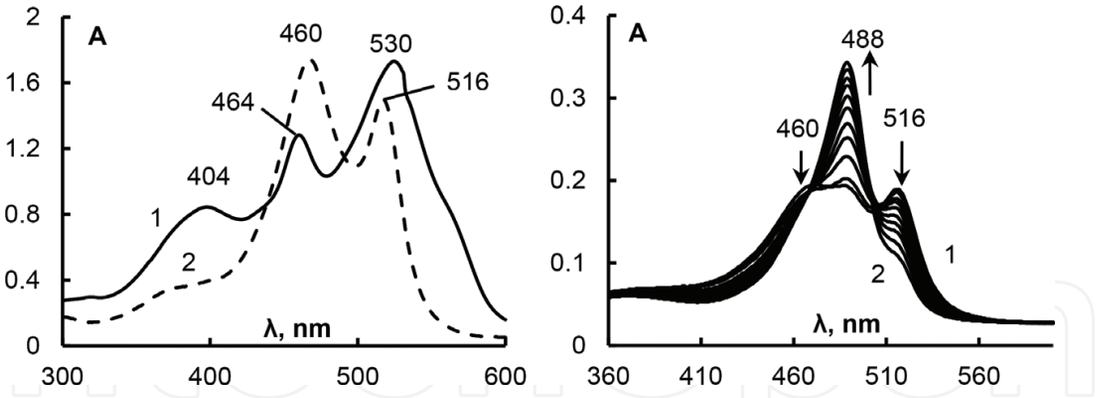

Figure 5. Left: [*Ni*(*dpm*)$_2$] (1) and [*Cu*(*dpm*)$_2$] (2) benzene solutions EAS; right: changes in [*Cu*(*dpm*)2] benzene solution EAS upon C_{AcOH} variation, M: 0.02 (1), 0.12 (2).

Unlike $\left[Cu(dpm)_2\right]$, the $\left[Ni(dpm)_2\right]$ formation is a kinetically controlled reaction which was found to take place with measurable rate in the acid concentrations range from $2.410 \cdot 10^{-4}$ to 0.2 M. Acid addition was found to provoke decrease in the 530 nm band with simultaneous increase in the H_2dpm^+ band at 493 nm (**Figure 6**). Whereas at the low acid concentrations ($\leq 2 \cdot 10^{-3}$), there were bands of heteroligand complex observable in the EAS, increase of the concentration led to a full dissociation lacking any complications.

Straight lines obtained in the semi-logarithmic coordinates suggest first-order reaction relative to complex concentration, described with the equation:

$$-\frac{dC_{\left[Ni(dpm)_2\right]}}{d\tau} = k_{obs} C_{\left[Ni(dpm)_2\right]} C_{AcOH}^2 \tag{18}$$

Each of the two equilibria could be described, therefore, as the consequent protonation of the dipyrromethene ligand. For an equilibrium involving formation of heteroligand complex

$$\left[Ni(dpm)_2\right] + 2AcOH = [Ni(dpm)(AcO)] + [H_2dpm](AcO) \tag{19}$$

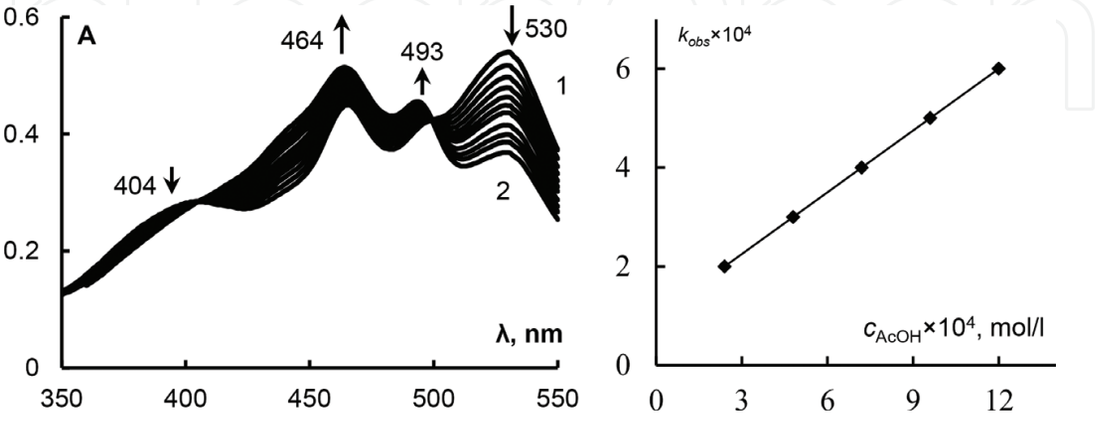

Figure 6. Left: changes in [*Ni*(*dpm*)$_2$] EAS upon acetic acid addition: 1—0 *min*; 2—reaction end; right: dependence of observable protolytic dissociation rate for [*Ni*(*dpm*)$_2$] relative to C_{AcOH}.

Kinetic scheme involves the following stages:

$$\begin{gathered}\left[Ni(dpm)_2\right] + AcOH \leftrightarrow \left\{Ni(dpm)_2(AcOH)\right\}^{\neq}, \quad k_1, slow \\ \left\{Ni(dpm)_2(AcOH)\right\}^{\neq} \rightarrow [Ni(dpm)(AcO)] + Hdpm, \quad k_2, fast \\ Hdpm + AcOH \rightarrow [H_2dpm](AcO), \quad k_3, fast\end{gathered} \tag{20}$$

For the heteroligand complex dissociation

$$[Ni(dpm)(AcO)] + 2AcOH = Ni(AcO)_2 + [H_2dpm](AcO) \tag{21}$$

And the kinetic scheme could be written as follows:

$$\begin{gathered}[Ni(dpm)(AcO)] + AcOH \leftrightarrow \{Ni(dpm)(AcO)(AcOH)\}^{\neq}, \quad k_1^*, slow \\ \{Ni(dpm)(AcO)(AcOH)\}^{\neq} \rightarrow Ni(AcO)_2 + Hdpm, \quad k_2^*, fast \\ Hdpm + AcOH \rightarrow [H_2dpm](AcO), \quad k_3, fast\end{gathered} \tag{22}$$

Observable second-order reaction relative to acid concentration suggests formation of the heteroligand complex to be the limiting stage of the process. Quasi-steady-state assumption along with concluded insignificance of heteroligand complex dissociation speed allows us to derive the equation:

$$-\frac{dC_{\left[Ni(dpm)_2\right]}}{d\tau} = \left(\frac{k_1k_2}{k_{-1}+k_2}\right) C_{\left[Ni(dpm)_2\right]} C_{AcOH}^2 \tag{23}$$

which is in good agreement with the experimentally derived equation:

$$k_{obs} = \frac{k_1k_2}{k_{-1}+k_2} \tag{24}$$

From the temperature variation experiments, activation parameters of the reaction were obtained.

T, K	k	E_a, kJ/mol	$\Delta S^{\neq}$, J/(mol·K)	$\Delta H^{\neq}$, kJ/mol
dpm$^-$ = 3,3′,4,5,5′-pentamethyl-4′-ethyl-2,2′-dipyrromethene anion				
298	0.29 ± 0.02	43.9 ± 2.7	−115.2 ± 12.7	41.4 ± 2.5
318	0.42 ± 0.03			
328	0.83 ± 0.05			
dpm$^-$ = 3,3′,5,5′-tetramethyl-4,4′-dibutyl-2,2′-dipyrromethene anion				
298	2279 ± 3	35 ± 3	−72.14 ± 13	32.5 ± 3.8
303	2660 ± 3			
313	4541 ± 5			
318	5272 ± 11			

Activation energy for the studied compound was found to be higher than that for the Ni(II) butyl-substituted dipyrrinate [15]. Strong inductive effect of alkyl moieties leads to higher electron-donating ability of the pyrrolic nitrogen and, therefore, increases kinetic stability of the compounds.

5. Patterns of BODIPY kinetic acid: Base dissociation

As it was mentioned before, understanding of a BODIPY behaviour in aggressive media is crucial within the scope of their practical application. The only data available to date was their higher solvolysis stability as compared to the d-metal dipyrrinates. Results reviewed below [25–28] thus are the first attempts of quantitative evaluation of a protolytic and solvoprotolytic resilience of a boron-dipyrromethenes.

6. Kinetical studies of BODIPY protolytic dissociation

Kinetic stability was evaluated for 4,4′-diethyl-3,3′,5,5′-tetramethyl-dipyrromethene ($Hdpm^1$), μ-phenyl-4,4′-diethyl-3,3′,5,5′-tetramethyl-dipyrromethene ($Hdpm^2$) and disodium 4,4′-disulpho-3,3′,5,5′-tetramethyl-dipyrromethene ($Hdpm^3$) difluoroborates. Studies were carried out in benzene, ethanol and water (both pure and mixed together) solutions. Acetic acid, trichloroacetic acid, trifluoroacetic acid, sulfuric acid and hydrogen chloride were used as protolysis agents.

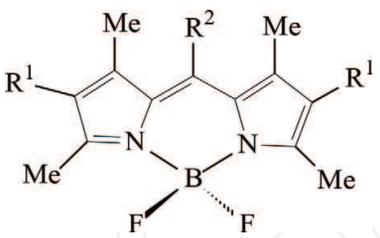

All of the compounds exhibited intense electronic absorption band at 528, 523 and 491 nm, respectively, and a charge-transfer band situated in a near UV region. Sulphonated complex exhibited hypsochromically shifted maximum due to the differences in electronic structure (**Figure 7**).

Electronic absorption and fluorescence spectroscopy data lacked any dissociation hallmarks for $\left[BF_2dpm^1\right]$ in benzolic and ethanolic solutions of acetic and trichloroacetic acid at 298 K. Neither did it in the pure corresponding acids. Heating followed by boiling for a time span of 20 to 30 minutes demonstrated absolute insusceptibility of a $\left[BF_2dpm^1\right]$ to acetic acid, whereas trichloroacetic acid evoked kinetically resolved decrease in the main absorption band at 528 nm with simultaneous raise of $[H_2L]^+$ characteristic band at 485 nm.

$\left[BF_2dpm^1\right]$ underwent dissociation in $EtOH\text{-}CF_3COOH$ and $EtOH\text{-}H_2SO_4$ solutions at 298 K with a speed sufficient for a ratiometric studies. $\left[BF_2dpm^2\right]$ showed itself to be way more volatile since dissociation was observed even in the $C_6H_6\text{-}CCl_3COOH$ solution at 298 K. Both

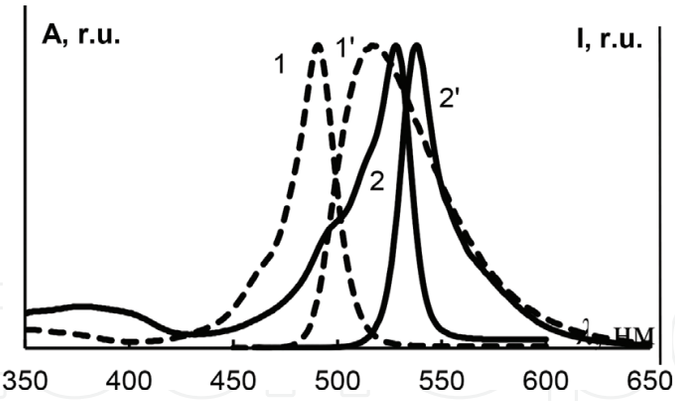

Figure 7. Electronic absorption (1, 2) and fluorescence (1′, 2′) spectra of $[BF_2dpm^2]$ and $[BF_2dpm^3]$ in EtOH and water.

protolytic and solvoprotolytic dissociation processes of the $\left[BF_2dpm^1\right]$ and $\left[BF_2dpm^2\right]$ complexes were found to yield the protonated form of the corresponding ligands $[H_2L]^+$. The water-soluble $\left[BF_2dpm^3\right]$ complex showed no hallmarks of dissociation in EAS in the 7–0 pH range (*HCl* aqueous). Overnight exposure to the lowest pH studied led to a very few, if any, changes in the electronic absorption spectrum of the compound. It was impossible to provoke $\left[BF_2dpm^3\right]$ kinetically resolved dissociation all the way up to the 2 M *HCl* concentration. The latter predictably yielded deprotonated form of the ligand $[H_2L]^+$.

To summarize, treatment of BODIPY with proton-donating agents leads to a fluorophore destruction down to a protonated ligand form. Protolytic or a solvoprotolytic destruction thus provokes significant changes in photophysical and spectral properties of the studied compounds due to destruction. Looking back to the technological aspects, irreversible changes in the dipyrrinates spectral characteristics after the sol-gel process should not have been erroneously described by the weak specific interactions [6, 7]. Instead, a way more pronounced dye destruction should have been taken into account.

Typical fluorescence and absorption changes observed during the dissociation process are presented below (**Figures 8** and **9**).

Formal kinetic analysis of a $\left[BF_2dpm^3\right]$ dissociation process reveals first order of the reaction relatively to the complex concentration. The observable rate constant, at the same time, is in a linear dependence from the H^+ ion activity:

$$k_{obs} = const \cdot a_{H^+} \tag{25}$$

Activities were calculated according to the literature data for an *HCl* aqueous solution [29, 30].

Kinetical equations of the second order are obviously applicable here:

$$-\frac{dC_{[BF_2dpm^{1,2}]}}{d\tau} = kC_{[BF_2dpm^{1,2}]}C_{HA} \qquad -\frac{dC_{[BF_2dpm^3]}}{d\tau} = kC_{[BF_2dpm^3]}C_{H^+} \tag{26}$$

Equations proposed along with the experimental data suggest one to assume the process to be the two-stage protonation of the complex as stated below:

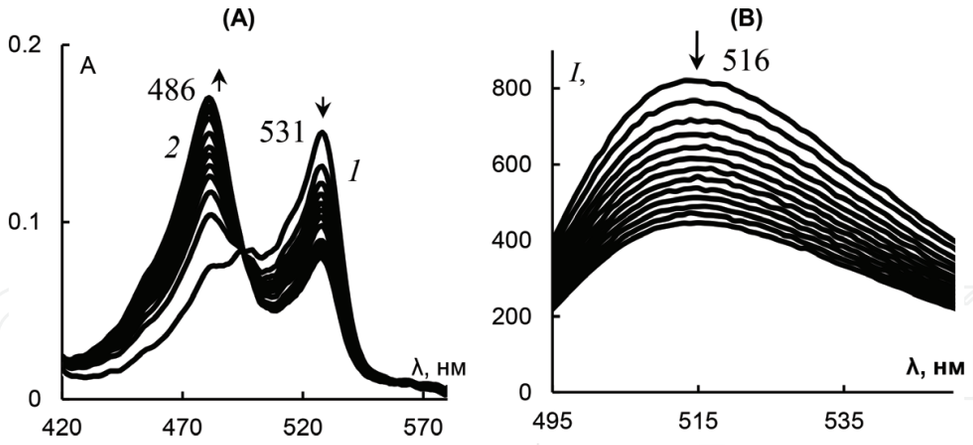

Figure 8. (A) Changes in EAS during [BF_2dpm^1] dissociation in *EtOH–CF*$_3$*COOH* binary mixture (C_{CF_3COOH} = 3.73 M at 298.15 K), t, s: 0 (1), 2700 (2); (B) decrease in fluorescence spectrum during [BF_2dpm^3] dissociation in *EtOH–*H_2SO_4 binary mixture.

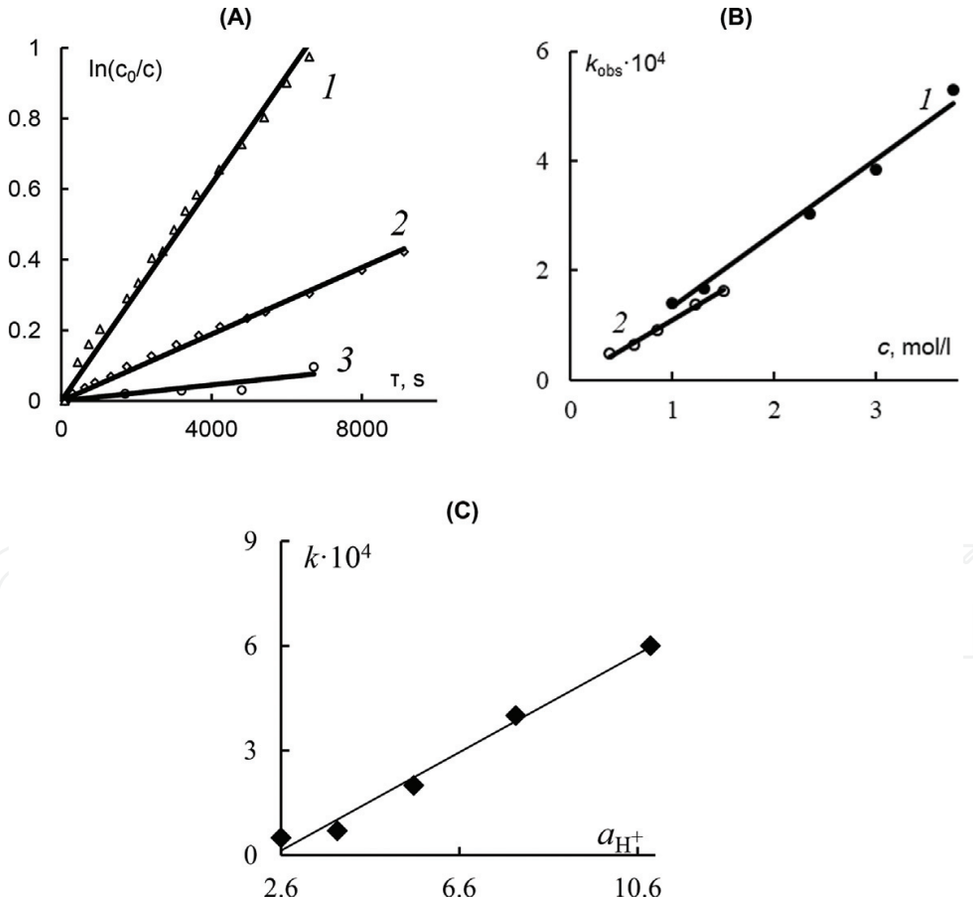

Figure 9. (A) Semi-logarithmic plot for the [BF_2dpm^1] dissociation in the *EtOH–CF*$_3$*COOH* binary mixture (T = 298.15 K), C_{CF_3COOH}, M: 0.384 (1), 0.62 (2), 1.23 (3); (B) changes in observable dissociation rate (k_{obs}) [BF_2dpm^1] relative to acid concentration in *EtOH*: 1, *CF*$_3$*COOH*; 2, H_2SO_4; (C) changes in observable dissociation rate (k_{obs}) [BF_2dpm^3] relatively to H^+ ion activity in aqueous *HCl*.

$$[BF_2dpm] + H^+\cdots A^- \leftrightarrow \left\{[BF_2dpm \cdot H]^+\cdots A^-\right\} \quad k_1, fast$$
$$\left\{[BF_2dpm \cdot H]^+\cdots A^-\right\} \rightarrow Hdpm + \left[BF_2^+\cdots A^-\right] \quad k_2, slow \tag{27}$$
$$Hdpm + H^+\cdots A^- \rightarrow [H_2dpm^+\cdots A^-] \quad k_3, fast$$

Quasi-steady-state assumption (suggesting that step 2 is rate-determining) allows stating the kinetical equation for this process in a convenient form:

$$-\frac{dC_{[BF_2dpm]}}{d\tau} = \left(\frac{k_1k_2}{k_{-1}+k_2}\right)C_{[BF_2dpm]}C_{HA}, \tag{28}$$

which totally coincides with the experimentally derived equation stated before.

Kinetic and activation parameters for the studied reaction are listed in the table below.

BODIPY dissociation thus proceeds via the S_E2 route. Unlike the protolytic destruction of d-metal dipyrrinates process, rigorously mediated by attack of donating nitrogen atom, BODIPY destruction process was found to possibly involve interaction between fluorine and electrophilic agent. Since such an ambiguity was hard to resolve experimentally, quantum chemical examinations were carried out. Examination of potential energy surfaces for both possible reaction routes allowed us to state fluorine protonation followed by the subsequent HF elimination to be the first stage of the process.

This fact by itself, however, does not influence the kinetic model of the process proposed above.

Compound	*T*, K	$k \cdot 10^3$, l/(mol·s)	E_a, kJ/mol	$\Delta H^{\neq}$, kJ/mol	$\Delta S^{\neq}$, J/(mol·K)
EtOH–CF_3COOH					
[BF_2dpm^1]	298	0.20 ± 0.01	—	—	—
EtOH–H_2SO_4					
[BF_2dpm^1]	298	0.10 ± 0.01	104 ± 6	102 ± 6	20 ± 1
	308	0.40 ± 0.02			
	318	1.4 ± 0.1			
C_6H_6–CCl_3COOH					
[BF_2dpm^2]	298	0.50 ± 0.03	—	—	—
EtOH–H_2SO_4					
[BF_2dpm^2]	298	0.050 ± 0.003	103 ± 6	101 ± 5	12.0 ± 0.6
	308	0.090 ± 0.005			
	318	0.70 ± 0.004			
H_2O–HCl					
[BF_2dpm^3]	298	0.070 ± 0.004	—	—	—

Ultimately, obtained results allow us to state a set of patterns for kinetic BODIPY protolytic dissociation stability. Both $\left[BF_2dpm^1\right]$ and $\left[BF_2dpm^2\right]$ are only susceptible to dissociation in benzolic solutions upon heating. Temperature increase leads to the 'monomer ↔ dimer'

equilibrium shift for carboxylic acids and to the decrease of the solvated proton activity [31]. Interestingly, whereas the pure CF_3COOH does not provoke $\left[BF_2dpm^1\right]$ dissociation, the presence of $EtOH_2^+$ particles in ethanolic solutions leads to reasonable solvoprotolysis rates at 298 K. Dissociation rate is also affected positively by the solution acidity as can be seen from the comparison of $EtOH\text{-}CF_3COOH$ and $EtOH\text{-}H_2SO_4$ systems above. The same pH solutions of $\left[BF_2dpm^1\right]$ and $\left[BF_2dpm^2\right]$ in $EtOH\text{-}H_2SO_4$ demonstrate the twice-reduced (for the latter) rate constant due to influence of the phenyl moiety on the nitrogen atom partial charge.

BODIPY, therefore, is unique in terms of kinetic stability towards protolytical and solvoprotolytical dissociation. Namely, different d-metal dipyrrinates in the C_6H_6–CH_3COOH solutions exhibit rate constants in the range from $0.6 \cdot 10^{-3}$ to $2.28 \cdot 10^3$ $l^2/(mol^2 \cdot s)$ or even demonstrate thermodynamically controlled equilibrium for the $Cu(II)$ complexes. Boron-dipyrromethenes, meanwhile, due to high B-N bond energy and pronounced chelating effect, are stable in similar conditions. As will be shown in the next section, BODIPYs also undergo the process of a protolytic dissociation by a mechanism, far different from the one occurring for dipyrrinates of d- and f-metals.

7. Quantum chemical modeling of protolytic dissociation mechanism

BODIPY, unlike d-metal dipyrrinates, has an ambiguity lying beneath the protolytic destruction mechanism due to specific coordination centre structure. In addition to the possibility of direct nucleophilic attack towards pyrrolic nitrogen, the phosphorus atom is also capable to interact with electrophilic agent with consequent *HF* elimination. Due to complexity of direct observation, quantum chemical investigation of potential energy surfaces for both of the possible protolytic dissociation mechanisms was performed.

Quantum chemical calculations were performed using GAUSSIAN03W and HyperChem 8.0.3 software. Semi-empirical PM6 method, which was verified basing on the experimental structural data for the bulky organic molecules, was used for rough geometry estimation and potential energy surface evaluation. Result refinement was performed using density functional theory approximation, with a B3LYP hybrid functional and a 6-31G(d,p) basis set.

The first studied mechanism involves direct nitrogen protonation with and consequent $B-N$ bond cleavage. On the other side, the second proposed mechanism involves formation of an $H-F$ hydrogen bond followed by *HF* elimination (**Figure 10**).

For potential energy surface cross sections, interatomic distance was chosen as an independent coordinate. Namely, those were $N-H$ bond length for the first mechanism and $F-H$ bond length for the second one.

Net Mulliken charges on the atoms show the favor for the second mechanism demonstrating fluorine to be more electron-rich than nitrogen. Optimized geometries for BODIPY and its single- and double-protonated forms are presented in **Figure 11**. Protonation of the atoms causes charge inversion on the fluorine atom and decrease of the partial positive charge on the pyrrolic nitrogen (**Table 1**).

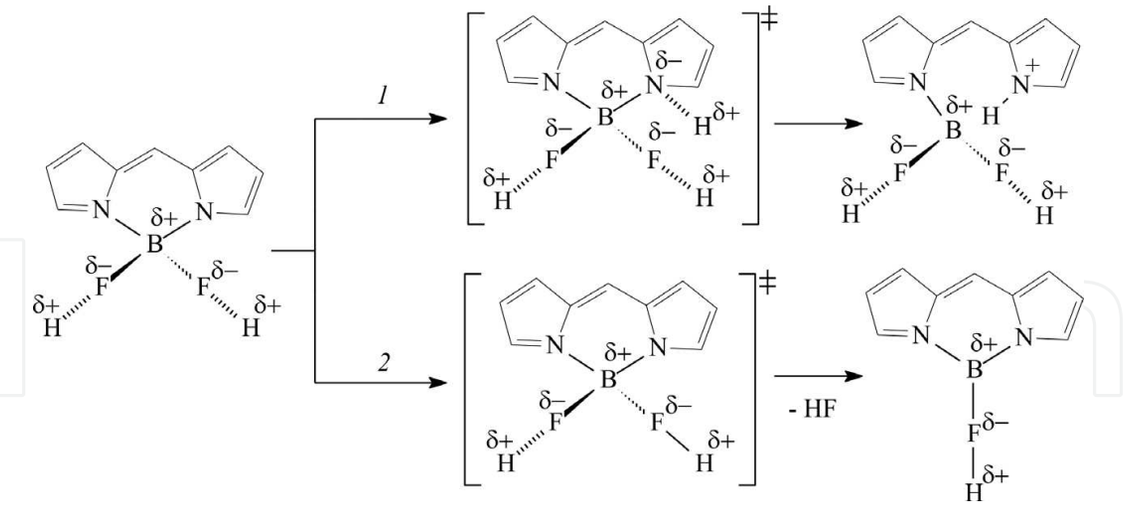

Figure 10. Proposed routes of BODIPY dissociation.

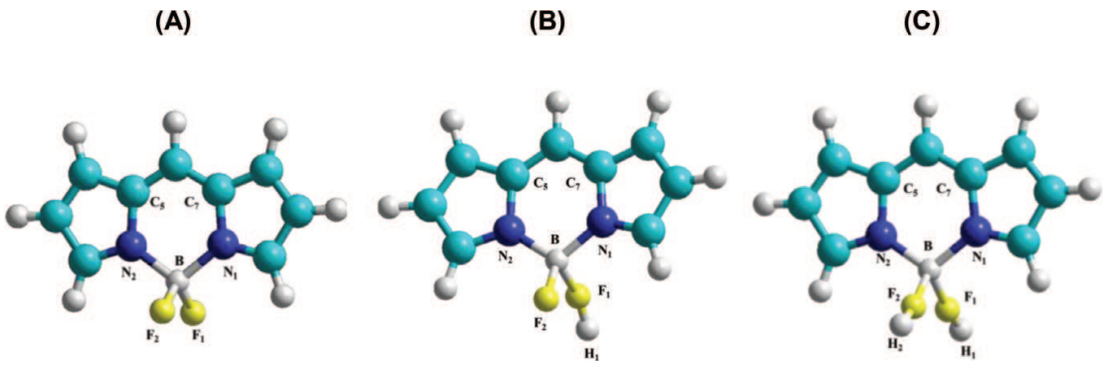

Figure 11. Optimized structures of BODIPY (A), single-protonated (B) and double-protonated (C) BODIPY forms.

Atom.	Structure		
	A	B	C
N_1	0.307	0.219	0.077
N_2	0.307	0.218	0.077
F_1	−0.21	0.052	0.072
F_2	−0.209	−0.158	0.071
B	0.06	0.13	0.021
H_1		0.307	0.323
H_2			0.323

Table 1. Net Mulliken atomic charges calculated using DF B3LYP/6-31G(d,p) approach.

$H-F$ bond length equilibrates near 0.957 Å with $B-F-H$ 155° bond angle. $B-F$ distance elongates upon interaction from 1.352 Å up to 1.521 Å with simultaneous $B-F$ order decrease from 0.97 down to 0.52. The latter explains ease of consequent destabilization and bond cleavage (**Figure 12**).

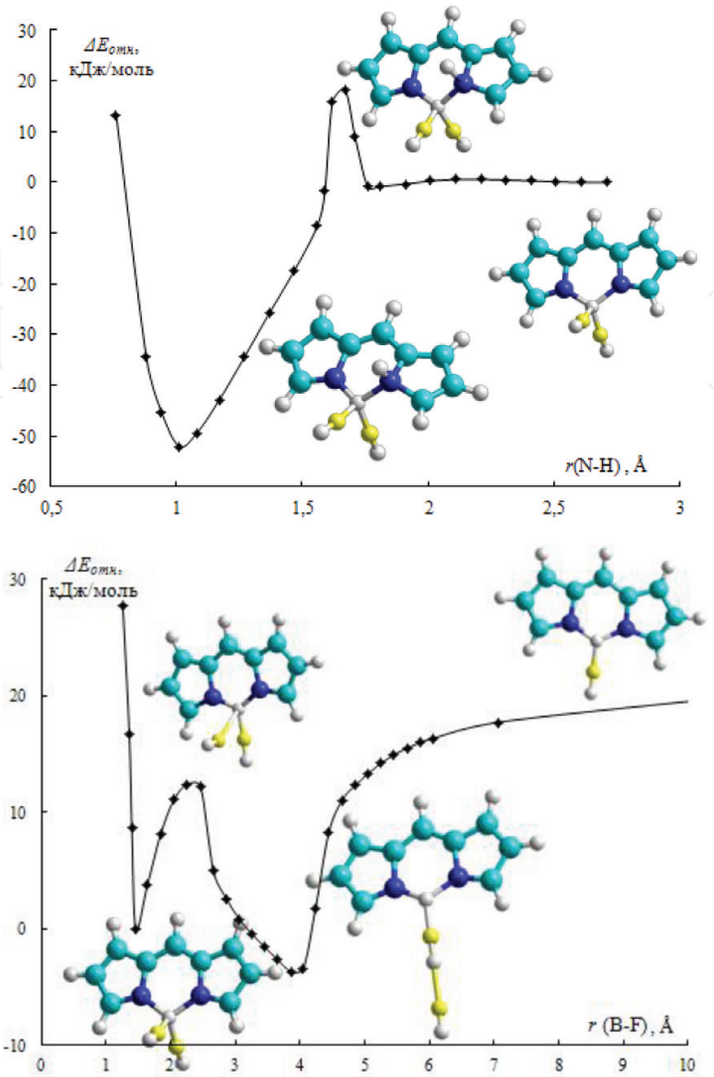

Figure 12. Potential energy surface cross sections for the first (top) and the second (bottom) mechanisms. ΔE (y axis) is calculated relatively to the stable BODIPY structure.

Activation energy for the nitrogen protonation corresponds to 18 kJ/mol. $N_1C_5C_7N_2$ dihedral angle increase from the fully planar ($\approx 0^\circ$) to a strongly twisted (15.6°) configuration occurs in this case.

For an *HF* elimination mechanism, there are two minima observed: the first one corresponds to the original BODIPY structure, whereas the second denotes trigonal coordination polyhedra of the complex as shown in the figure. Geometry of the transition state for this mechanism undergoes no pronounced changes except the obvious $B-F-H$ angle increase and $H-F$ bond tightening. The activation energy for this case estimates 12 kJ/mol mostly owing to the $B(III)$ coordination polyhedra change. Alas, the trigonal geometry is only possible in vacuo, since acid ligands will force back the tetrahedral shape in the condensed phase.

From the aforementioned we state that fluorine protonation with consequent *HF* elimination is the most probable mechanism of the first stage of BODIPY protolytic dissociation. This still corresponds to the kinetic model proposed above while nicely explaining outstanding stability of boron-dipyrromethenes to protolytic dissociation.

http://dx.doi.org/10.5772/intechopen.80498

8. Hydrolysis and destruction of BODIPY in alkaline solutions

Resilience of BODIPY to the aggressive components of the reaction mixtures involved in the hybrid material formation is of high importance. Up to our first paper in the field [26], stability of boron-dipyrromethenes in the alkaline medium was never studied. Here we review kinetic stability of disodium 4,4′-disulpho-3,3′,5,5′-tetramethyl-dipyrromethene ($Hdpm^3$) difluoroborate $[BF_2dpm]$ in the aqueous $NaOH$ solutions.

$[BF_2dpm]$ aqueous solutions exhibited intense absorption peak at 491 nm. There were very few, if any, changes in electronic absorption spectra upon pH increase from 7 up to 9, even after 24 h of exposure.

First, changes were observed at pH values ≥10—absorption maximum decrease was accompanied by the growth of 206 nm band, corresponding to the monopyrrolic products. Further, pH increase in the 10–12 range increased destruction rate dramatically (**Figure 13**).

Linearization using first-order reaction coordinates yields unity root mean square and approves the first-order reaction relative to the complex concentration. At the same time, dependence of k_{obs} from pOH suggests the second-order reaction relative to OH^- ion.

Acid (HCl) addition leads to full recovery of the photophysical characteristics, suggesting reversibility of the first stage of interaction studied. Thus, the first stage is the formation of unstable anionic ligand form, which consequently breaks down to yield monopyrrolic products. The suggested reaction scheme is presented below:

$$[BF_2dpm]^{2-} + 2OH^- \leftrightarrow \left[BF_2(OH)_2\right]^- + dpm^{3-} \quad k_1$$

$$dpm^{3-} \rightarrow colorless\ pyrroles \quad k_2 \tag{29}$$

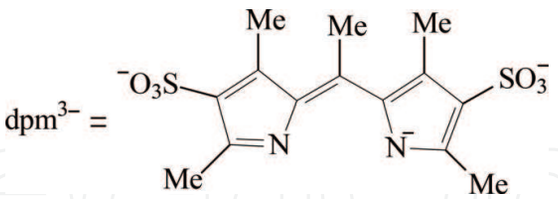

According to the scheme, the canonical kinetic equation could be written as

$$\frac{-dC_{BF_2dpm}}{d\tau} = k_{obs}C_{[BF_2dpm]} \tag{30}$$

Quasi-steady-state assumption for this reaction scheme allows stating the kinetical equation for this process in a form:

$$k_{obs} = \left(\frac{k_1k_2}{k_{-1}}\right)C^2_{(OH^-)} \tag{31}$$

which coincides with the experimentally obtained dependencies. Thus, total reaction rate equation could be written as

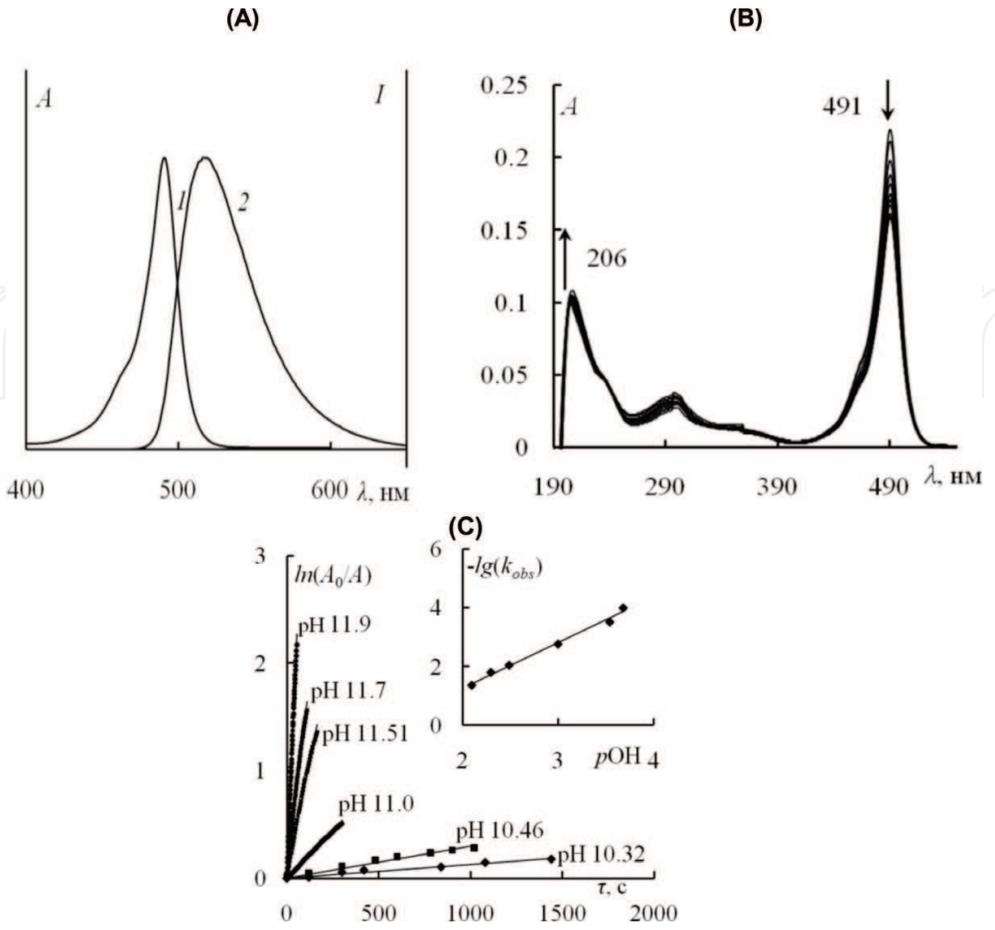

Figure 13. (A) Electronic absorption (1) and fluorescence (2) spectra of an aqueous [BF_2dpm] solution (pH 7.0); (B) changes in [BF_2dpm] EAS upon *NaOH* addition at 298 K; (C) kinetical data on [BF_2dpm] destruction at 298 K. (B inset) changes in solution absorbance relatively to the *pOH*.

$$\frac{-dC_{BF_2dpm}}{d\tau} = \left(\frac{k_1 k_2}{k_{-1}}\right) C_{[BF_2dpm]} C^2_{(OH^-)} \tag{32}$$

Ultimately, we can state high BODIPY stability towards alkaline medium, granting possibility of their usage in high pH range during hybrid materials synthesis. Proposed mechanism and data obtained for the hydrolytic BODIPY destruction in alkaline medium extends the frontiers of their practical applications, suggesting proper usage of acidic additives preventing boron-dipyrrin destruction.

9. Conclusions

Results reviewed in this chapter broaden the data on kinetic stability of dipyrrinates in acidic media. Introduction of the alkyl moiety to the ligand structure leads to an increase in the electron density near pyrrolic nitrogen atoms. Demonstrated results state decrease in stability

of intermediate complex upon alkyl chain length increase due to attenuation of +I effect impact. Kinetic stability of dipyrrinates is mainly affected by potency of interaction between electron-donating nitrogen atoms and acid molecules. This possibility, in turn, is highly susceptible to dipyrrin substituents amount, position and electron-donating behaviour. Central atom nature not just simply determines stability of the complex towards protolytic dissociation but fundamentally changes route of the process. Relative stability was stated for $Zn(II)$ and $Ni(II)$ dipyrrinates. The latter demonstrates formation of heteroligand complexes in the process of dissociation. $Pd(II)$ complexes have way higher stability and are only susceptible to dissociation in the trifluoroacetic acid solution. Outstanding stability is demonstrated by the boron difluoride dipyrromethenes, mostly due to the high $B-N$ bond energy and highly pronounced chelating effect. Quantum chemical investigations state that unlike that of d- and f-metal dipyrrinates, the first stage of BODIPY protolytic dissociation is fluorine protonation with consequent *HF* cleavage.

Investigation of the BODIPY destruction in aqueous alkaline medium suggests the first stage of the process to be the alkaline hydrolysis. Unstable intermediate anionic form of the ligand consequently decays yielding uncoloured monopyrrolic products. Analysis of the spectrophotometric data for the process is in good agreement with the reaction scheme proposed.

There is an ongoing research [32–36] on bis-dipyrrins protolytic dissociation stability. Generally, they are more labile, and benzene solutions of acetic acid are used for the investigation. Doubling the number of the electron-donating groups per molecule complicates the examination; however, with some assumptions made (such as synchronous protolysis) kinetical equations look quite similar with the ones derived in this chapter. It could be stated that lability of helicates (bis-dipyrrins binuclear complexes) in protolysis reactions also do increase if there are no any substituents in terminal pyrrole rings.

Author details

Yuriy S. Marfin*, Sergey D. Usoltsev and Evgeniy V. Rumyantsev

*Address all correspondence to: marfin@isuct.ru

Ivanovo State University of Chemistry and Technology, Ivanovo, Russian Federation

References

[1] Rumyancev EV, Marfin YS. Variacii struktury i supramolekulyarnogo okruzheniya kak sposoby vliyaniya na spektral'nye i fotofizicheskie harakteristiki kompleksov dipirrinov. In: XII Mezhdunarodnaya konferenciya «Spektroskopiya koordinacionnyh soedinenij». Tuapse; 2015. pp. 86-87 (Russian)

[2] Bersuker IB. Elektronnoe stroenie i svojstva koordinacionnyh soedinenij. In: Bersuker IB, editor. Vvedenie v teoriyu. 3-e izd, pererab. L.: Himiya; 1986. 287 p. (Russian)

[3] Berezin BD, Lomova TN. Reakcii dissociacii kompleksnyh soedinenij. M.: Nauka; 2007. 278 p (Russian)

[4] Grinberg AA. Vvedenie v himiyu kompleksnyh soedinenij. Izd. 3-e, pererab. i dop. M.: Himiya; 1966. 631 p (Russian)

[5] Kukushkin VY. Teoriya i praktika sinteza koordinacionnyh soedinenij. Akademii Nauk SSSR, Otd-nie fizikohimii i tehnologii neorgan. materialov. L.: Nauka; 1990. 260 p (Russian)

[6] Kukushkin YN. Himiya koordinacionnyh soedinenij. M.: Vyssh. shk.; 1985. 456 p (Russian)

[7] Kuznecova RT. Spektroskopicheskie i lazernye harakteristiki novyh effektivnyh lyuminoforov dlya shirokoj oblasti spektra na osnove kompleksov proizvodnyh dipirrolilmetena s diftorboratom. In: Kuznecova RT, Aksenova YV, Solodova TA, Bashkircev DE, Kopylova TN, Tel'minov EN, Majer i dr GV, editors. Optika i spektroskopiya. Vol. 115. No. 5. 2013. p. 797 (Russian)

[8] Aksenova YV. Fotonika i primenenie novyh lyuminoforov na osnove kompleksov dipirrolilmetenov. In: Aksenova YV, Kuznecova RT, Berezin MB, editors. Izvestiya Samarskogo nauchnogo centra Rossijskoj akademii nauk. Vol. 17. No. 2. 2015. pp. 56-59 (Russian)

[9] Aksenova YV. Spektroskopicheskoe izuchenie fotofizicheskih i fotohimicheskih svojstv koordinacionnyh kompleksov dipirrinov. In: Aksenova YV, Kuznecova RT, Berezin MB, Pavich TA, Arabej SM, editors. V knige: XXV S'ezd 304 po spektroskopii molodezhnaya nauchnaya shkola po optike i spektroskopii: sbornik tezisov. Moskva. 2016. pp. 66-67 (Russian)

[10] Marfin YS. Polimernye kompozicii, soderzhashchie bordipirrinovye lyuminofory. In: Marfin YS, Rumyancev EV, editors. V Vserossijskaya s mezhdunarodnym uchastiem konferenciya i shkola dlya molodyh uchenyh «Makromolekulyarnye nanoob'ekty i polimernye nanokompozity», g. Moskva; 2015. p. 89 (Russian)

[11] Banuelos J, Lopez Arbeloa F, Arbeloa T, Salleres S, Vilas JL, et al. Journal of Fluorescence. 2008;**18**(5):899

[12] Guseva GB. Vzaimodejstviya s rastvoritelyami linejnyh oligopirrol'nyh soedinenij i ih metallokompleksov. In: Guseva GB, Antina EV, Berezin MB, V'yugin AI, Balanceva EV, editors. ZHurn. fiz. himii. Vol. 76, No. 9. 2002. pp. 1595-1599 (Russian)

[13] Semejkin AS. Vzaimosvyaz' stroeniya i sol'vatacionnyh harakteristik alkilzameshchennyh dipirrolilmetenov, ih oksa- i tioanalogov. In: Semejkin AS, Berezin MB, CHernova OM, Antina EV, Syrbu SA, Lyubimova TV, Kutepov AM, editors. Izvestiya AN. Ser. him. No. 8. 2003. pp. 1712-1718 (Russian)

[14] Helevina OG. Kineticheskaya ustojchivost' kompleksov tuliya(III) i samariya(III) s oktafeniltetraazaporfirinom v sredah na osnove uksusnoj kisloty. In: Helevina OG, Miroshnichenko YS, Kabesheva EV, Kulinich VP, SHaposhnikov GP, editors. ZHurnal obshchej himii. Vol. 74. No. 12. 2004. pp. 1937-1941 (Russian)

[15] Rumyantsev EV, Marfin YS. Protolytic dissociation mechanisms and comparative acid. Stability of palladium(II), zinc(II), copper(II), and nickel(II) complexes of alkylated dipyrrins. Transition Metal Chemistry. 2014;**39**:699-704

[16] Guseva GB. Reakcionnaya sposobnost' α,α-dipirrolilmetena v reakciyah s nekotorymi kompleksami Co(II) i Cu(II). In: Guseva GB, Antina EV. Koord. Himiya; Vol. 32, No. 7. 2006. pp. 541-546 (Russian)

[17] Rumyancev EV. Kompleksy dipirrolilmetenov: faktory stabilizacii i fiziko-himicheskie svojstva. In: Rumyancev EV, Antina EV, Desoki A, editors. Sb.: Trudy XXIV Mezhdunarodnoj CHugaevskoj konferencii po koordinacionnoj himii i Molodezhnoj konferencii-shkoly «Fiziko-himicheskie metody v himii koordinacionnyh soedinenij». St. Peterburg. 2009. pp. 358-359 (Russian)

[18] Hammet LP, Deyrup AJ. Journal of the American Chemical Society. 1932;**54**:2721

[19] Stewart R, O'Donnell JP. Journal of the American Chemical Society. 1962;**84**:493-494

[20] Gammet L. Osnovy fizicheskoj organicheskoj himii. M.: Mir; 1972 (Russian)

[21] Olah A. Journal of Organic Chemistry. 2005;**70**:2413-2429

[22] Guseva GB. Termodinamika reakcij kompleksoobrazovaniya medi(II), cinka(II), kobal'ta (II), rtuti(II) I nikelya(II) S α,α-dipirrolilmetenom v dimetilformamide. In: Guseva GB, Antina EV, Berezin MB, V'yugin AI. Koordinacionnaya Himiya. Vol. 30, No. 1. 2004. pp. 32-35 (Russian)

[23] Klyueva ME. Proyavlenie makrociklicheskogo effekta v processe dissociacii kompleksov Zn2+ i Mn3+ s protoporfirinom: krat. soobshcheniya. In: Klyueva ME, Lomova TN, Berezin BD, editors. ZHurn. fiz. himii. Vol. 62, vyp. 12. 1988. pp. 3341-3344 (Russian)

[24] Klyueva ME. Vliyanie strukturnyh faktorov na kinetiku i mehanizm dissociacii marganec (III)tetrafeniloporfirinov v sernoj kislote. In: Klyueva ME, Lomova TN, Berezin BD. Tez. dokl. IV Vsesoyuz. soveshch. 305 «Probl. sol'vatacii i kompleksoobrazovaniya v rastvorah», Ivanovo, 6–8 iyunya 1989 g. Ivanovo, Ch. I. 1989. p. 44 (Russian)

[25] Pang W. Modulating the singlet oxygen generation property of meso-β directly linked BODIPY dimers. In: Pang W, Zhang X-F, Zhou J, Yu C, Hao E, et al. Chemical Communications, Cambridge, England. Vol. 48. 2012. pp. 5437-5439

[26] Rumyancev EV. Koordinacionnaya himiya dipirrolilmetenov i ih proizvodnyh: Fundamental'nye aspekty i prakticheskie prilozheniya. In: Rumyancev EV, Antina EV, editors. V sb. tezisov dokladov XXV Mezhdunarodnoj CHugaevskoj konferencii po koordinacionnoj himii i II Molodezhnoj konferencii-shkoly «Fiziko-himicheskie metody v himii koordinacionnyh soedinenij». 6–11 iyunya 2011. g., Suzdal'. pp. 31-32 (Russian)

[27] Rumyancev EV. Gidroliz i destrukciya borftoridnogo kompleksa dipirrolilmetena v shchelochnyh rastvorah. In: Rumyancev EV, Aleshin SN, editors. Izvestiya VUZov. Himiya i himicheskaya tehnologiya. Vol. 56, No. 2. 2013. pp. 67-70 (Russian)

[28] Rumyancev EV. Reakcii protoliticheskoj dissociacii dipirrolilmetenatov medi(II) i nikelya (II) v benzol'nyh rastvorah uksusnoj kisloty. In: Rumyancev EV, Aleshin SN, Antina EV, editors. ZHurnal obshchej himii. Vol. 83, No. 10. 2013. pp. 1738-1742 (Russian)

[29] Rumyantsev EV, Alyoshin SN, Marfin YS. Kinetic study of bodipy resistance to acids and alkalis: Stability ranges in aqueous and non-aqueous solutions. Inorganica Chimica Acta. 2013;**408**:181-185

[30] Rumyancev EV. Kvantovo-himicheskoe modelirovanie nachal'nyh stadij protoliticheskoj dissociacii borftoridnogo kompleksa dipirrolilmetena. In: Rumyancev EV, Marfin YS, Aleshin SN, editors. Izvestiya vysshih uchebnyh zavedenij. Seriya: Himiya i Himicheskaya Tehnologiya; Vol. 56, No. 9. 2013. pp. 18-22 (Russian)

[31] Robinson R, Stoks R. Rastvory elektrolitov. M.: 1963. 647 p (Russian)

[32] Guseva GB, Antina EV, Berezin MB. Kinetics of the dissociation of transition metal complexes with α,α-dipyrrolylmethene in acetic acid-benzene as a binary proton-donating solvent. Russian Journal of Coordination Chemistry. 2003;**29**(10):690-693

[33] Guseva GB, Antina EV, Ksenofontov AA, V'yugin AI. Kineticheskaya model' i mehanizm kislotnoj dissociacii bis(dipirrolilmetenatov) dmetallov. Kinetika i kataliz. 2014;**55**(4):411 (Russian)

[34] Antina LA, Guseva GB, V'yugin AI, Antina EV. Kineticheskaya ustojchivost' kompleksov ryada d-metallov s 3,3'-bis(dipirrolilmetenom) v binarnom protonodonornom rastvoritele uksusnaya kislota-benzol. ZHurnal obshchej himii. 2012;**82**(7):1195-1200 (Russian)

[35] Antina LA, Guseva GB, V'yugin AI, Antina EV. Kinetika reakcij dissociacii kompleksov cinka(II) s 3,3-bis(dipirrolilmetenami) v binarnom rastvoritele uksusnaya kislota-benzol. ZHurnal fizicheskoj himii. 2012;**86**(11):1759 (Russian)

[36] Stid DV, Etvud DL. Supramolekulyarnaya himiya. Vol. 2 t. M.: Akademkniga; 2007. 480 p (416 p, Russian)